LA-13513-MS
Approved for public release;
distribution is unlimited.

General Heat Transfer Characterization and Empirical Models of Material Storage Temperatures for the Los Alamos Nuclear Materials Storage Facility

Los Alamos
NATIONAL LABORATORY

Los Alamos National Laboratory is operated by the University of California for the United States Department of Energy under contract W-7405-ENG-36.

An Affirmative Action/Equal Opportunity Employer

LA-13513-MS

UC-721
Issued: October 1998

General Heat Transfer Characterization and Empirical Models of Material Storage Temperatures for the Los Alamos Nuclear Materials Storage Facility

J. D. Bernardin
W. S. Gregory

Los Alamos
NATIONAL LABORATORY
Los Alamos, New Mexico 87545

TABLE OF CONTENTS

Abstract ---------- 1

Nomenclature ---------- 2

1. Introduction ---------- 3

2. Experimental Methods ---------- 5

3. Results ---------- 8

    3.1 General Heat Transfer Characterization ---------- 10

    3.2 Qualitative Characterization of Influential Heat Transfer Parameters ---------- 10

    3.3 Empirical Models for Material Storage Temperature Predictions ---------- 18

    3.4 Validation and Use of Empirical Correlations ---------- 20

4. Conclusions ---------- 23

References ---------- 24

Appendix ---------- 25

General Heat Transfer Characterization and Empirical Models of Material Storage Temperatures for the Los Alamos Nuclear Materials Storage Facility

by

J. D. Bernardin and W. S. Gregory

Abstract

The Los Alamos National Laboratory's Nuclear Materials Storage Facility (NMSF) is being renovated for long-term storage of canisters designed to hold heat-generating nuclear materials. A fully passive cooling scheme, relying on the transfer of heat by conduction, free convection, and radiation, has been proposed as a reliable means of maintaining material at acceptable storage temperatures. The storage concept involves placing radioactive materials, with a net heat-generation rate of 10 W to 20 W, inside a set of nested steel canisters. The canisters are, in turn, placed in holding fixtures and positioned vertically within a steel storage pipe (6.10 m length, 45.7 cm outer diameter, and 1.27 cm wall thickness). Several hundred drywells are arranged in a linear array within a large bay and dissipate the waste heat to the surrounding air, thus creating a buoyancy driven airflow pattern that draws cool air into the storage facility and exhausts heated air through an outlet stack.

In this study, an experimental apparatus was designed to investigate the thermal characteristics of simulated nuclear materials placed inside two nested steel canisters positioned vertically on an aluminum fixture plate and placed inside a section of steel pipe. The heat-generating nuclear materials were simulated with a solid aluminum cylinder containing an embedded electrical resistance heater. Calibrated type T thermocouples (accurate to ±0.1°C) were used to monitor temperatures at 20 different locations within the apparatus.

The purposes of this study were to observe the heat dissipation characteristics of the proposed canister/fixture plate storage configuration, to investigate how the storage system responds to changes in various parameters, and to develop and validate empirical correlations to predict material temperatures under various operating conditions.

NOMENCLATURE

Symbol	Description
k	Thermal conductivity
P	Power dissipation
$\dot{q}$	Volumetric heat generation rate
r	Radius
T	Temperature

Subscript	Description
dw	Drywell
mat	Material
o	Outer
s	Surface

1. INTRODUCTION

The Los Alamos Nuclear Materials Storage Facility (NMSF) is currently being renovated for long-term storage of heat-generating nuclear materials. Continuous heat generation of the radioactive materials, combined with prescribed storage temperature limits, requires a well devised and reliable cooling technique that does not interfere with other storage requirements (i.e., operation, handling, security, safety, etc.). To achieve this goal, a passive cooling scheme that relies on free convection and radiation heat transfer has been proposed.

The NMSF storage and cooling system concepts are shown schematically in Figure 1. The storage concept involves placing radioactive materials, with a net heat generation rate of 10 W to 20 W, inside a set of nested steel canisters. The canisters are, in turn, placed in holding fixtures and positioned vertically within a steel storage pipe (6.10 m length, 45.7 cm outer diameter, and 1.27 cm wall thickness), referred to as a drywell. Several hundred drywells are arranged in a linear array within a large bay and dissipate the waste heat to the surrounding air. The passive cooling strategy relies on the transfer of heat by conduction, convection, and radiation from the stored material, through the nested canisters and holding fixtures, and out to the drywell. The heated drywells create a buoyancy driven airflow pattern that draws cool air into the storage facility and exhausts heated air through an outlet stack.

In this study, an experimental apparatus was designed to investigate the thermal characteristics of simulated nuclear materials placed inside two nested steel canisters positioned vertically on an aluminum fixture plate and placed inside a section of steel pipe. The purposes of this investigation were to observe the heat dissipation characteristics of the proposed storage and cooling system configuration, perform a parametric study to investigate how the system responds to changes in different variables, and to develop empirical correlations to predict material temperatures under various operating conditions. The empirical models developed in this study will serve as a link between material storage temperatures and drywell and facility air temperatures, the latter two of which are currently being investigated in full-scale NMSF bay experiments and numerical models.

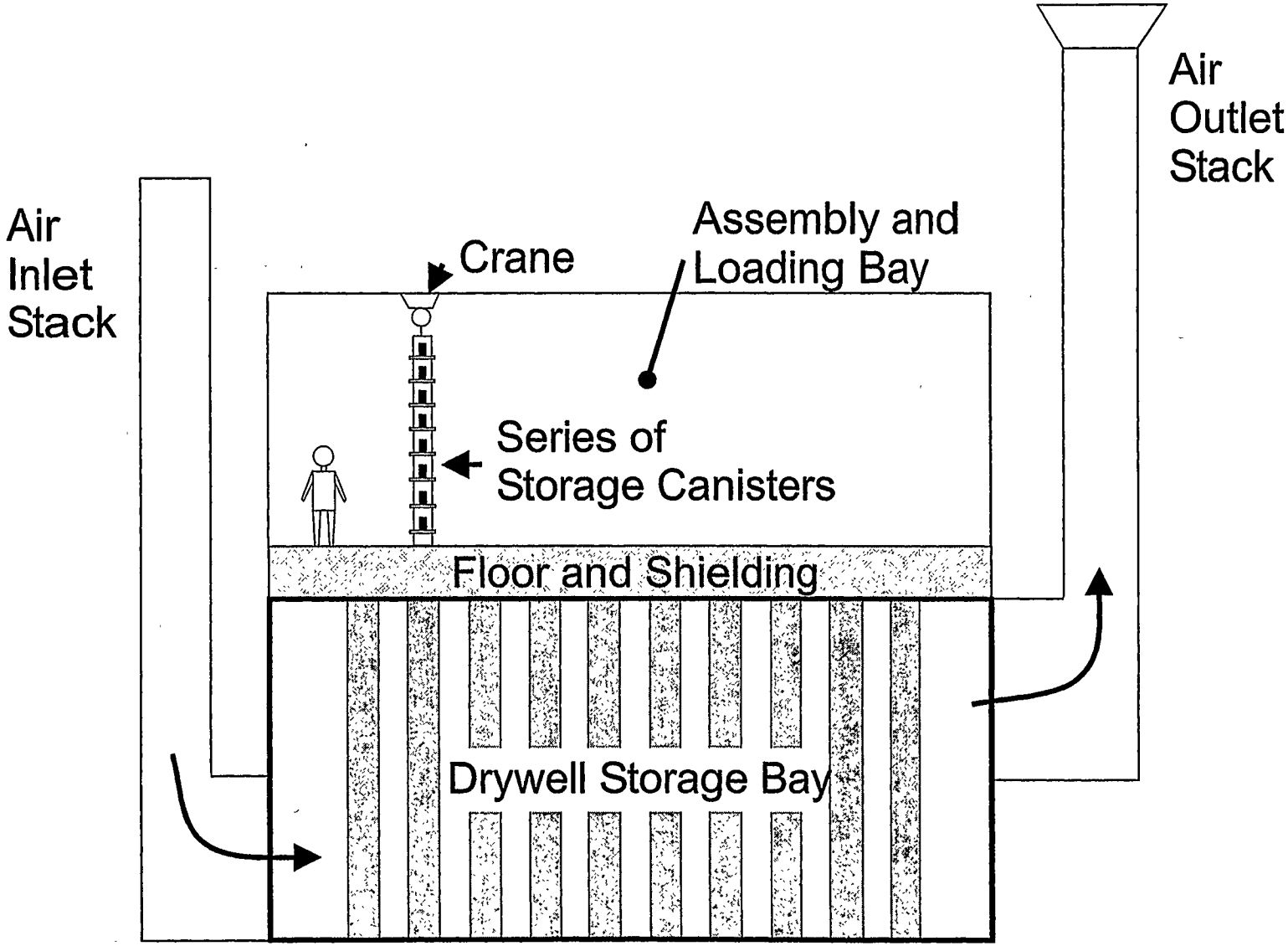

Figure 1. Conceptual design of the Los Alamos Nuclear Materials Storage Facility.

2. EXPERIMENTAL METHODS

The NMSF single nested canister experimental apparatus is displayed in Figure 2. The apparatus was designed to investigate the thermal characteristics of simulated nuclear materials placed inside two nested steel canisters positioned vertically on an aluminum fixture plate and placed inside a section of steel pipe. It should be mentioned that, while the results of this study are applicable to most types of nuclear materials, the primary focus of this investigation was associated with plutonium metal.

The heat-generating nuclear materials were simulated with a solid aluminum cylinder containing an embedded electrical resistance heater. A cylindrical shaped material was chosen because it served as a realistic geometry and provided a low surface-area-to-volume ratio, an attribute that resulted in conservative heat dissipation characteristics. The majority of the materials to be stored in the NMSF will possess much more complex geometries with larger surface-area-to-volume ratios, thus resulting in higher heat transfer rates by conduction to the canister and convection to the canister gas. Consequently, the aluminum cylinders, when insulated from direct contact with the storage canisters, represent a near worst-case storage geometry that will give conservative material storage temperatures.

Aluminum cylinders with an outer diameter of 5.08 cm and lengths of 15.24, 13.34, and 8.89 cm were used in this study to simulate nuclear material. The longest of these cylinders was selected to correspond in size to heated cylinders used in previous NMSF experiments in which multiple heated canisters were stored in a full-scale drywell [1, 2, 3]. This material size matching provided a link between the current single nested canister experiments and the previous realistic storage investigations so that validation and utilization of empirical material temperature prediction techniques could be demonstrated. The remaining two cylinders, with lengths of 13.34 cm and 8.89 cm, were chosen to correspond to equivalent volumes of plutonium generating a total of 15 W and 10 W, respectively. These values correspond to a heat-generation rate of 2.83 W/kg, which is suitable for aged plutonium. By insulating the aluminum cylinder from direct contact with the inner storage canister, the surface temperatures of the cylinder will be nearly identical to those obtained with an actual plutonium cylinder of equivalent

geometry. The material temperatures measured in this study correspond to the surface temperatures of the aluminum cylinders. However, it can be shown using the one-dimensional steady-state radial heat-conduction equation

$$T(r)=\frac{\dot{q}\,r_o^2}{4k}\left[1-\left(\frac{r}{r_o}\right)^2\right]+T_s \tag{1}$$

and the thermal conductivity of plutonium, 6.74 W m^{-1} K^{-1}, that the centerline and surface temperatures of a plutonium cylinder with an outer diameter of 5.08 cm are within 1.3 K of one another. Consequently, the material temperatures reported in this study correspond to an average plutonium storage temperature.

In all tests, the aluminum cylinders were positioned vertically in the storage canisters. In most cases, the cylinders were insulated from the inner canister bottom by a 1.6 mm thick G-10 insulating spacer, while in a few tests, the bottom surfaces of the aluminum cylinders were allowed to make direct contact with the canister. Heat was supplied to the aluminum cylinders by an electrical resistance cartridge heater connected to a variable ac voltage supply. The power to the aluminum cylinder was determined by measuring the voltage drop and electrical resistance across the cartridge heater.

The aluminum cylinder was placed inside two nested steel canisters, the general dimensions of which are given in Figure 2. A gas transport line, connecting the sealed canisters to a roughing vacuum pump and compressed gas cylinders, allowed the effects of different canister fill gasses to be studied. The canisters were placed vertically on a cylindrical aluminum fixture plate as shown in Figure 2. The flat-bottom steel canisters and the solid aluminum fixture plates used in this study were selected using results of a previous investigation that explored the thermal performances of different canister and fixture plate geometries [4]. An upper fixture plate located immediately above the storage canisters was heated with several electrical resistance heaters to represent a realistic upper boundary condition that the nested canisters would be exposed to in a fully loaded drywell. The two fixture plates were fastened to four threaded rods to allow the effective canister spacing to be varied. The fixture plates and canister assemblies were

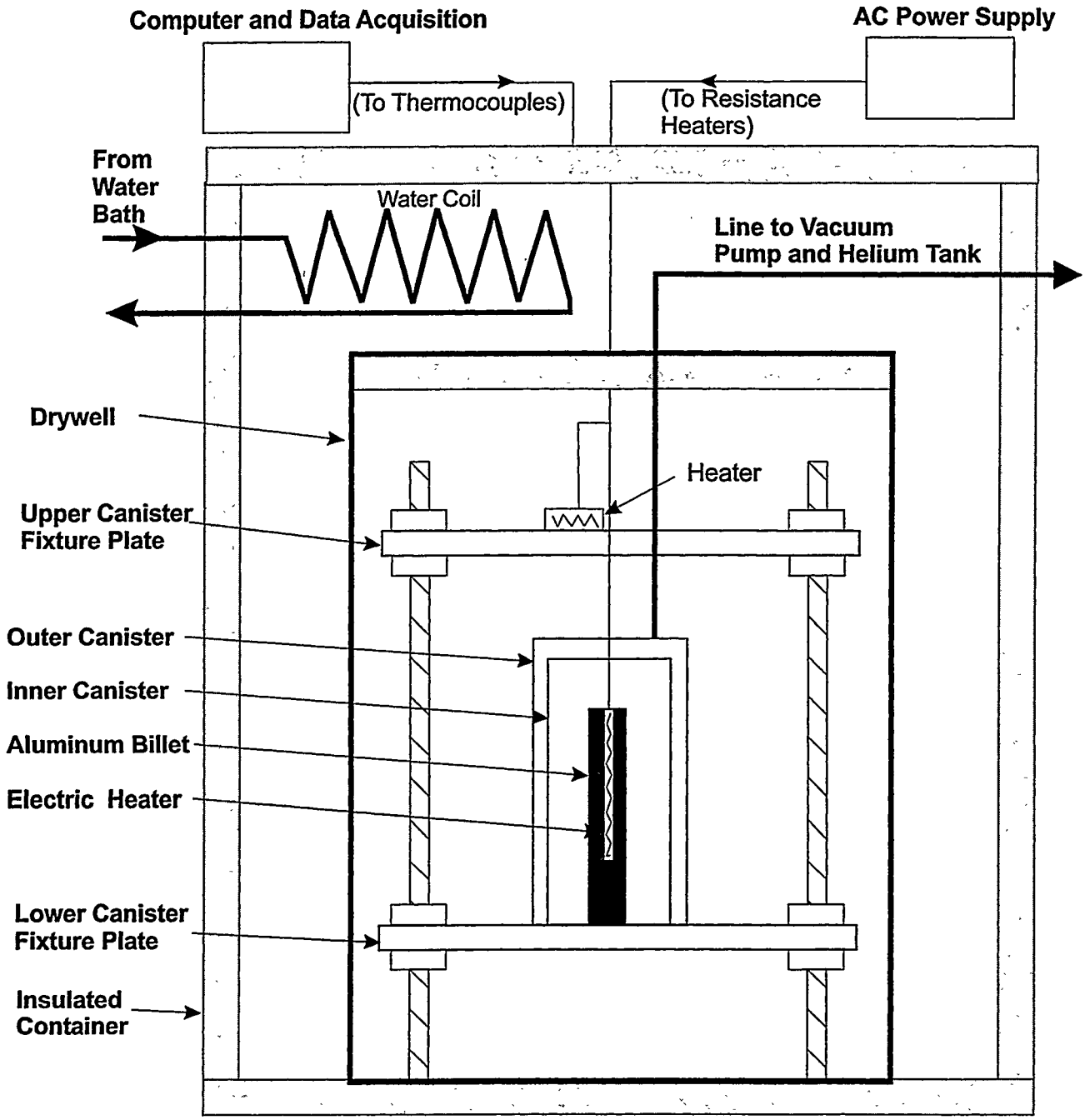

General Dimensions (cm)

Drywell	Inner Canister
Length = 61.0	Length = 24.1
O.D. = 45.7	O.D. = 11.4
Wall thickness = 1.27	Wall thickness = 0.16
Fixture Plate	Outer Canister
O.D. = 40.6	Length = 25.4
Thickness = 1.27	O.D. = 12.7
	Wall thickness = 0.16

Figure 2. Schematic diagram of the NMSF single nested canister experimental apparatus.

placed vertically within a 61 cm long drywell segment. This entire apparatus was then placed inside an insulated container formed from 2.54 cm thick foam insulating walls. A water chiller coil and electrical resistance heaters were used to control the air temperature within the insulated container and external to the drywell. This entire experimental apparatus was designed to represent a single nested canister segment of an actual drywell containing multiple storage canisters.

Calibrated type T thermocouples (accurate to ±0.1°C), connected to a Hewlett-Packard HP34970A data acquisition unit, were used to monitor temperatures at the various locations depicted in Figure 3.

The experiments were initiated by setting the ac voltage supply to deliver the necessary power to the resistance heater in the aluminum cylinder (10, 15, or 20 W). Next, the desired fill gas (either helium or air) was introduced into the nested canisters. The power to the upper fixture plate resistance heaters was manipulated until the steady-state temperature profiles on the upper and lower fixture plates were approximately equal. Approximately 8 to 10 hours were required to establish thermal equilibrium, after which the temperature data was recorded. Each test configuration was conducted for three different external drywell air temperatures, which were manipulated with the temperature controls mentioned previously. Several cases were repeated to ensure reproducibility.

3. RESULTS

The results of this study are presented in four sections. First, the general heat transfer characteristics of the nested canister/fixture plate storage scheme are presented. The second section includes a qualitative characterization of the effects of the following parameters on the material and canister temperatures: heat-generation rate, canister fill gas, external air temperature, thermal contact resistance, and canister spacing. The next section uses a more quantitative approach to analyze the material storage temperature. In particular, empirical correlations to predict material storage temperatures are presented for various storage configurations. The accuracy and usefulness of these correlations are

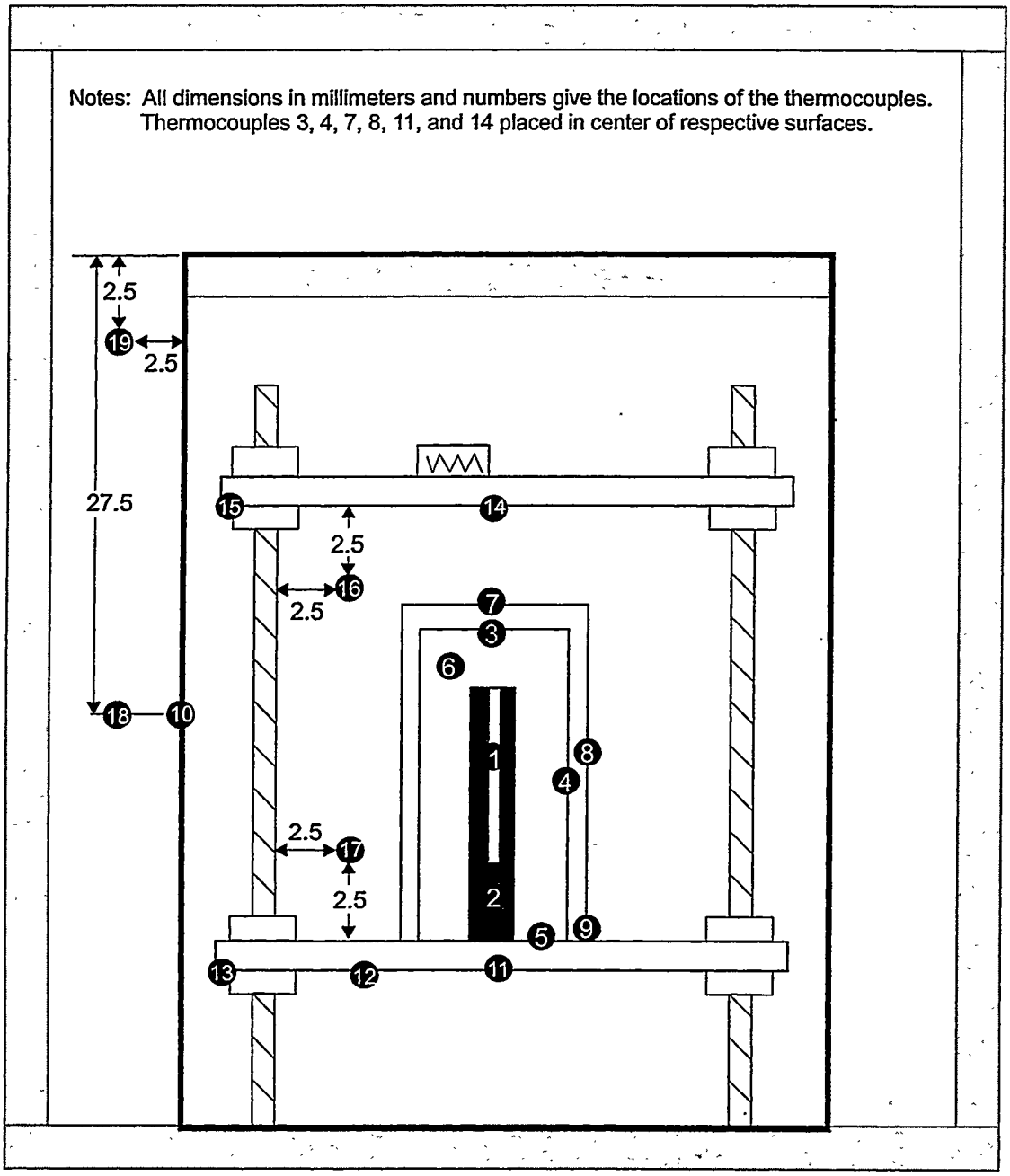

Figure 3. Schematic diagram of the thermocouple locations on the single nested canister experimental apparatus.

demonstrated in the final section using empirical data from previously conducted thermal experiments with a fully loaded drywell [3, 5].

3.1 General Heat Transfer Characterization

As discussed previously, the nested canister experiment was designed to represent a segment of a fully loaded drywell. The solid fixture plates used in this experiment effectively prevent the buoyant heated air of a nested canister set from reaching the canisters immediately above it. Consequently, this design feature has the net effect of dividing the drywell into a series of individual compartments or zones that transport the majority of the canister heat radially outward to the drywell wall.

The general heat dissipation from the nested canister storage configuration is shown schematically in the temperature contour plot of Figure 4 for a heat dissipation rate of 15 W and an external air temperature of 30°C. The temperature contours were approximated from discrete temperature measurements taken during the present study, as well as numerical model predictions from a previous investigation [1]. While these temperature contours are only approximate, they do allow one to identify heat paths and relative temperature magnitudes.

The largest temperature drop, and hence the greatest thermal resistance, is seen to exist between the material and the inner storage canister. Since no thermal insulation resistance exists between the material and the inner canister bottom, roughly half (based on surface area and temperature) of the heat is conducted out of the canisters and into the lower fixture plate. The remaining heat is conducted through the canister gas (air, in this case) to the outer canister surface. The heat from the fixture plate and the outer canister is eventually transferred to the drywell by circulating free convection and radiation.

3.2 Qualitative Characterization of Influential Heat Transfer Parameters

During the course of this study, several variables were found to influence the material storage temperatures. These variables included the heat-generation rate, canister fill gas, external air temperature, thermal contact resistance, and canister spacing. In the discussion that follows, all temperature data (except where noted) corresponds to a

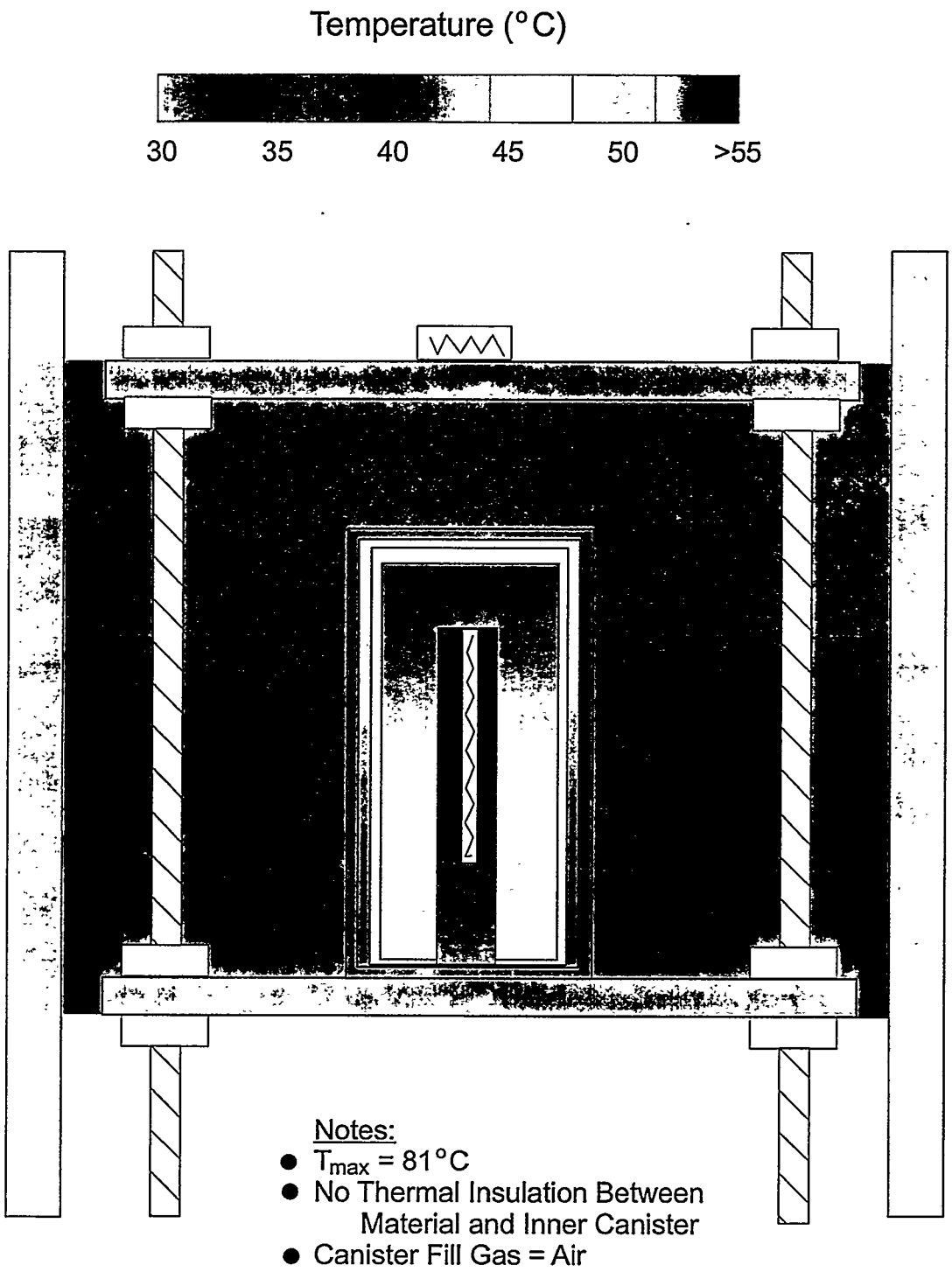

Figure 4. Temperature contours displaying the general heat distribution within the NMSF single nested canister experimental apparatus for a material heat-generation rate of 15 W and an external (to drywell) air temperature of 30°C. Note that this representation is only qualitative and the temperature values are approximate.

material geometry consisting of the aluminum cylinder, 15.24 cm in length and 5.08 cm in diameter.

Figure 5 displays the effects of heat-generation rate and canister fill gas on the material, outer canister side wall, and drywell surface temperatures. For the data of Figures 5(a) and 5(b), the total power was varied between 10 W and 20 W, which (for the cylinder volume considered) corresponds to a mass heat-generation rate between 1.68 W/kg and 3.35 W/kg for plutonium. For the total power range considered in this study, the component temperatures are seen to increase nearly linearly with increasing power, with a maximum worst-case material temperature value of 113°C. Helium gas has a thermal conductivity that is roughly eight times greater than that of air. Consequently, it was expected that helium would be a much more efficient gas than air as a canister fill gas in minimizing the material storage temperature. This expectation is indeed supported by the data in Figure 5, which shows that the material was roughly 10°C to 15°C cooler when stored in a helium environment rather than in air. As an interesting side note, the outer canister and drywell temperatures were relatively insensitive to the type of canister fill gas used. This makes sense when one recognizes that the canister fill gas only influences the thermal resistance inside the canister. Thus, if the total heat dissipation rate and the thermal resistance outside of the canisters remain constant, the temperature drop from the outer canister to the environment must remain constant.

Figure 6 shows that for a given total material power dissipation of 15 W, the material, outer canister, and drywell surface temperatures were found to increase in a linear fashion with increasing external drywell air temperature.

The effect of thermal contact resistance between the material and the inner canister is displayed in Figure 7(a), where the material, outer canister side wall, and drywell surface temperatures are plotted versus total material power dissipation. Relative to the case in which the material was allowed to make direct contact with the inner canister bottom, the material storage temperature increased 12°C at a material power dissipation of 10 W and 18°C at 20 W when a G-10 insulating spacer was placed between the material and the inner canister. The outer canister and drywell surface temperatures

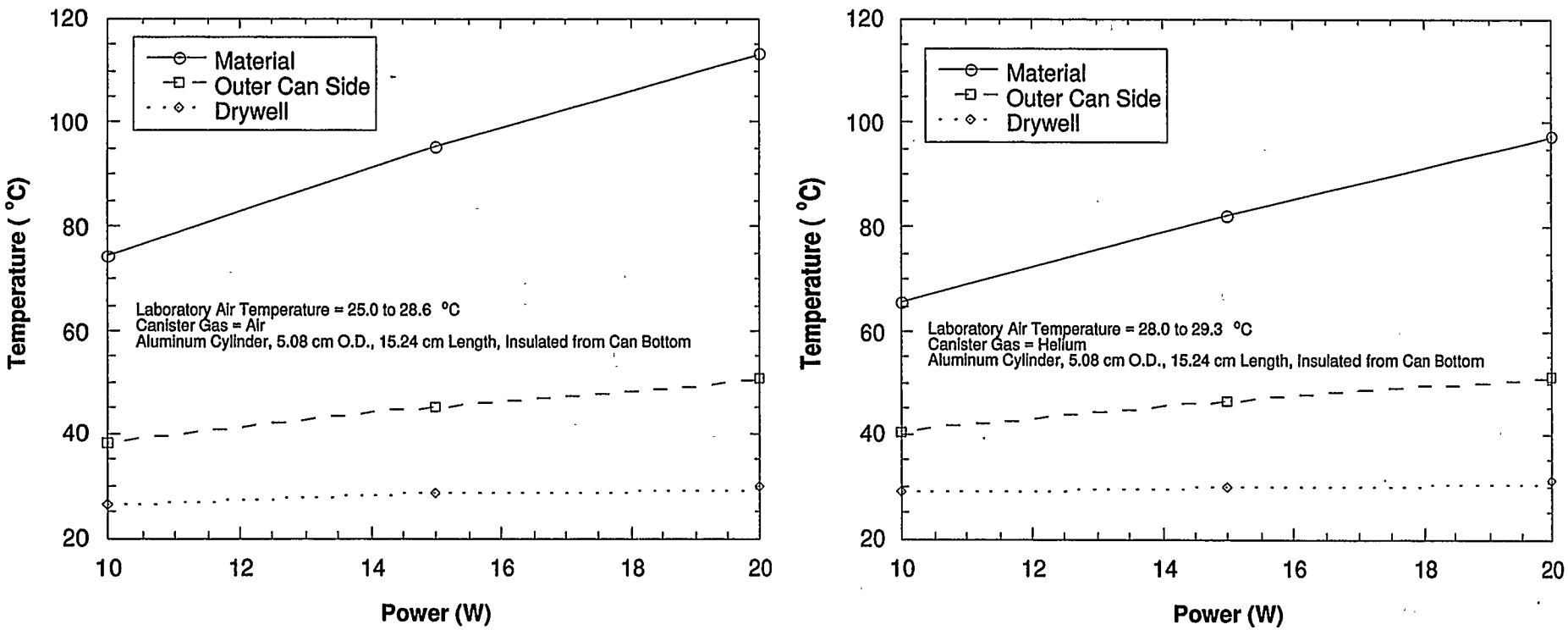

(a) (b)

Figure 5. Material, outer canister side, and drywell temperatures as a function of total material power for a 30.5 cm canister spacing and a G-10 insulating spacer between the material and inner canister, and for canister fill gases of (a) air and (b) helium.

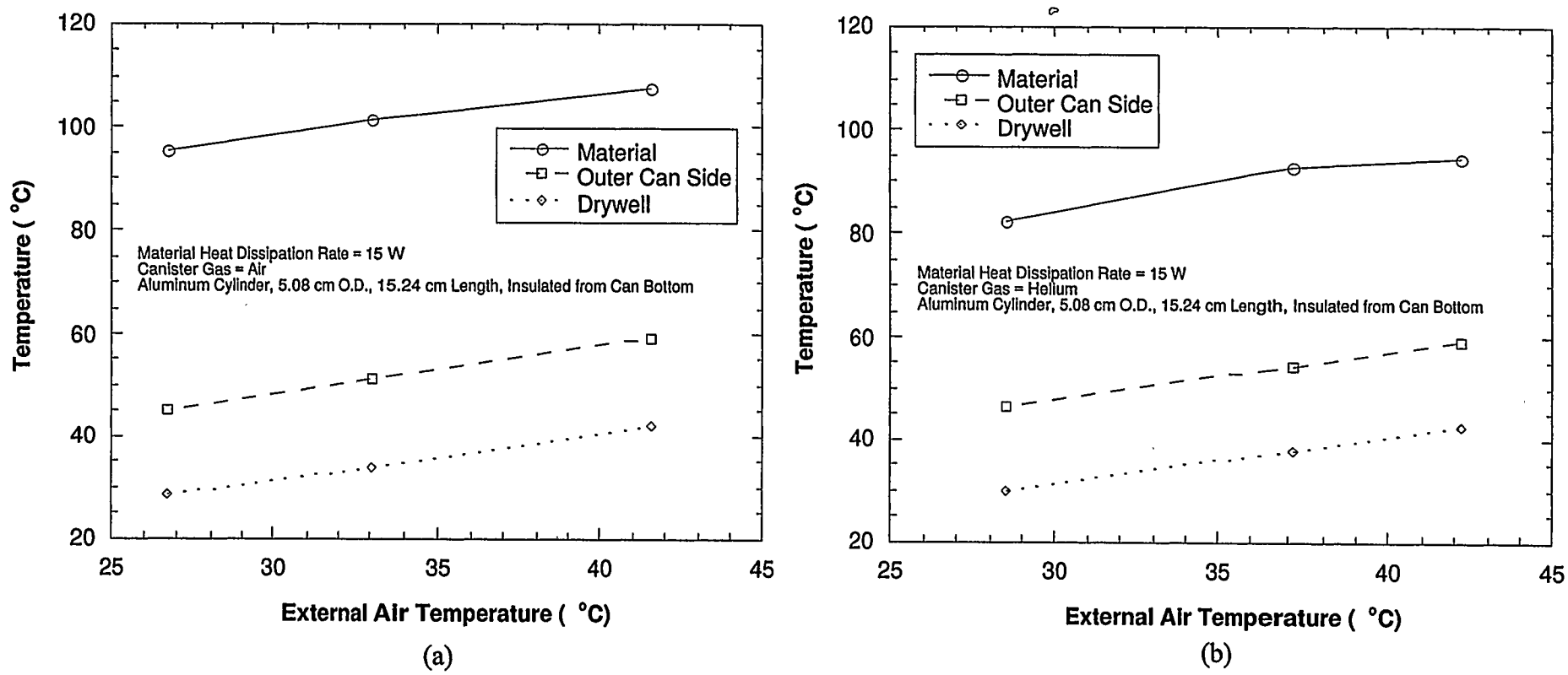

Figure 6. Material, outer canister side, and drywell temperatures as a function of external air temperature for a 30.5 cm canister spacing and a G-10 insulating spacer between the material and inner canister, and for canister fill gases of (a) air and (b) helium.

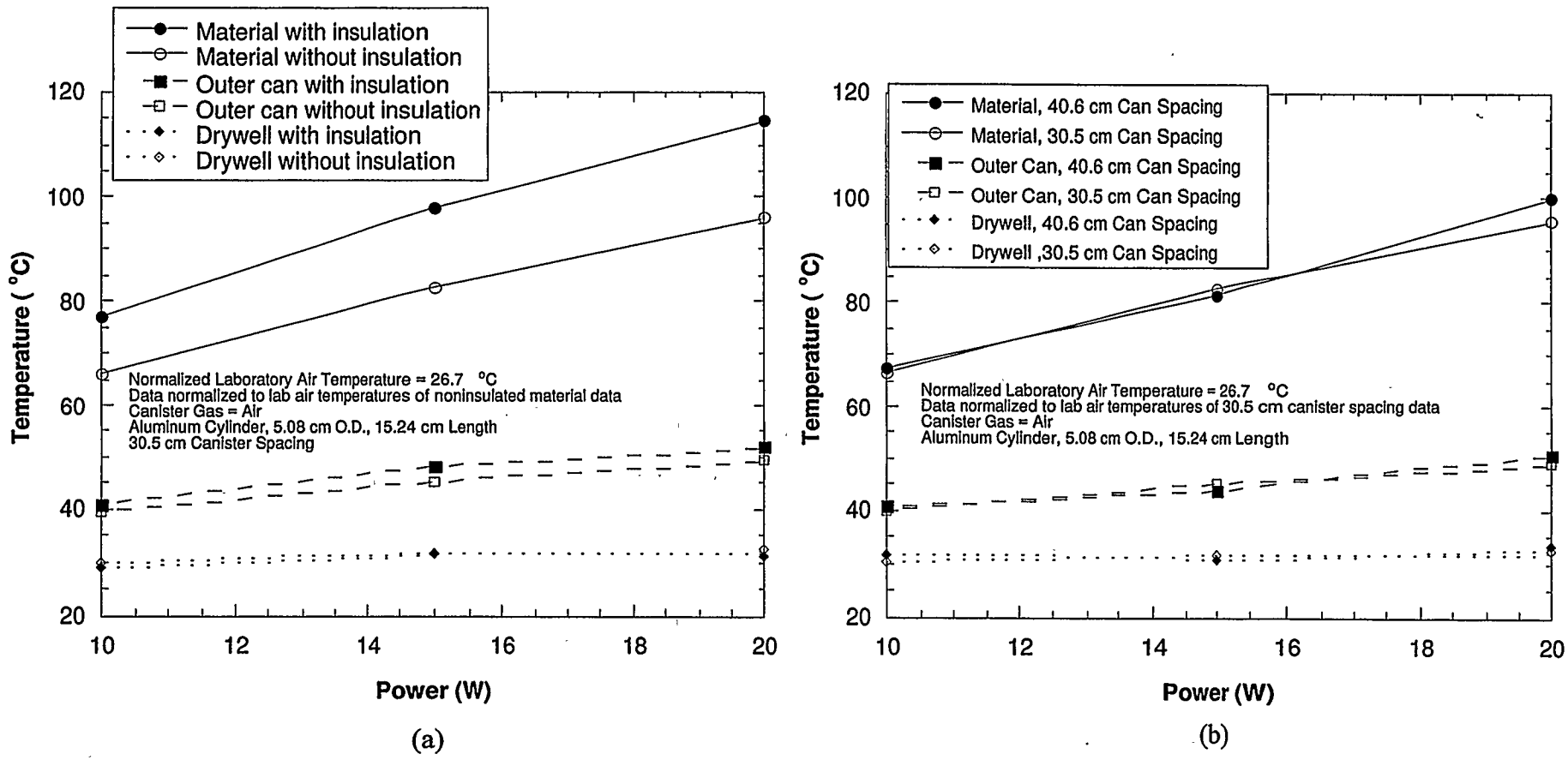

Figure 7. Material, outer canister side, and drywell temperatures as a function of total material power for (a) insulated versus non insulated materials and (b) 30.5 cm. versus 40.6 cm canister spacings.

were found to be less sensitive to material insulation. Temperature measurements indicated that the center of the lower fixture plate and the bottom of the outer canister were consistently within 1°C of one another, suggesting that the thermal contact resistance between the outer canister and the fixture plate is negligible.

Figure 7(b) indicates that the material and canister temperatures were relatively insensitive to canister spacing over the range studied.

The laboratory air temperature varied a few degrees between the tests used to create Figures 7(a) and 7(b). Consequently, to make accurate comparisons, all component temperatures were normalized to a laboratory air temperature of 26.7°C. This normalization required adding or subtracting the temperature difference between the true laboratory air temperature and the normalized value, to the component temperature.

A comprehensive summary of the effects of the various parameters on material storage temperatures is given below in Table 1.

Table 1. Qualitative summary of the effects of various parameters on material storage temperature.

Parameter	Effect on Material Storage Temperature
Heat Generation Rate	• For a given material geometry and size, material temperature increased nearly linearly with increasing volumetric heat-generation rate over the range encountered in this investigation (32.4 KW/m^3 to 64.8 KW/m^3). • The maximum material temperature increase was nearly 40°C when the total material power dissipation was increased from 10 W to 20 W in the 15.24 cm long aluminum cylinder. • For a given volumetric heat-generation rate, material temperature increased with increasing material volume (for a cylinder of a diameter of 5.08 cm).
Canister Fill Gas	• Material temperatures were reduced significantly (10°C to 15°C) by reducing the molecular weight of the canister fill gas. (That is, helium has a thermal conductivity which is roughly eight times higher than that of air). • Outer canister and fixture plate temperatures were relatively insensitive to changes in canister fill gas.
External (to drywell) Air Temperature	• Material temperature increased nearly linearly with increasing external air temperature over the range encountered in this investigation (24°C to 45°C).
Thermal Contact Resistance	• Improving the thermal contact between the material and inner canister significantly reduced the material temperature. Removing a G-10 insulating spacer from between the aluminum cylinder bottom and the inner canister reduced the material temperature by 10°C to 20°C. • The thermal contact resistance between the outer canister and fixture plate was minimal, as determined from the small temperature differences between these components for various tests.
Canister Spacing	• Increasing the canister spacing from 30.5 cm to 40.6 cm did not result in any appreciable change in the canister or material temperatures.

3.3 Empirical Models for Material Storage Temperature Predictions

The extensive temperature data base generated in this study was used to develop several empirical correlations to predict steady-state material storage temperatures from knowledge of the drywell surface temperature in the vicinity of the material and the total material heat-generation rate. These empirical tools will be employed in ongoing NMSF experiments and numerical models by providing a link between material and drywell temperatures, thereby eliminating the need for complex detailing of multiple storage canisters and materials.

Two different correlation forms were used to correlate material temperature to drywell temperature and total material heat-generation rate. For the temperature data corresponding to the 15.2 cm long aluminum cylinder, in which the total material heat-generation rate was varied, the following correlation form was employed to predict the average material temperature, T_{mat}:

$$T_{mat} = a T_{dw}^{b} P^{c}, \tag{2}$$

where T_{dw} is the average temperature of the drywell section around the material and single canister set of interest, P is the total material heat dissipation rate, and a, b, and c are empirical constants.

For the temperature data corresponding to the 8.9 cm and 13.3 cm long cylinders, the total material heat-generation rates were fixed at 10 W and 15 W, respectively. Consequently, a simple linear curve fit was deemed appropriate to correlate the relation between material and drywell temperatures:

$$T_{mat} = a T_{dw} + b. \tag{3}$$

The final forms of the correlations given by Equations (2) and (3) are summarized in Table 2. Each correlation corresponds to a particular material geometry, canister fill gas, material/canister interface condition, and total material heat-generation rates.

Several limiting conditions are imposed on the material temperature correlations and caution must be exercised in their use. First, the correlations correspond to the particular storage configuration shown previously in Figure 2. Next, a cylindrical material geometry was used to acquire the temperature data. This geometry, when insulated from direct contact with the inner canister, represents a near worst-case storage condition from a material storage temperature standpoint. The cylindrical geometry possesses a surface-area-to-volume ratio that is significantly lower than the typical materials planned for storage in the NMSF, and thus the cylinder should display a higher and more conservative storage temperature. Consequently, the temperature correlations given in Table 2 are expected to represent upper boundary, or worst-case, material storage temperatures. In addition, the correlations correspond to various total material heat-generation rates. For example, the 15.2 cm long cylinder correlations were developed for heat-generation rates ranging from 1.68 W/kg and 3.35 W/kg for plutonium metal, which corresponds to the 10 W to 20 W total material heat-generation rate range for the particular geometry. The correlations related to the 8.9 cm and 13.3 cm long cylinders, corresponding to 10 W and 15 W of total material heat-generation rates, respectively, were developed for a fixed heat generation rate of 2.8 W/kg, which is most realistic for aged plutonium. Finally, the material temperature was found to be highly dependent on the canister fill gas, which for this study, was either air or helium. Although helium provides significantly lower material temperatures than air does, it has a higher leak rate from poorly sealed vessels. Thus, for conservative estimates, it may be advantageous to use the correlations corresponding to the air fill gas rather than those corresponding to helium in order to predict long-term material storage temperatures.

Table 2. Summary of empirical correlations for predicting material storage Temperatures.

Cylinder Length (cm)	Canister Fill Gas	Storage Conditions and Parametric Ranges	Material Temperature Correlation (°C)
15.2	Air	• Material insulated from canister bottom • 10 W < P < 20 W • 25°C < T_{dw} < 50°C	$T_{mat} = 8.077 T_{dw}^{0.306} P^{0.534}$ (4)
15.2	Helium	• Material insulated from canister bottom • 10 W < P < 20 W • 25°C < T_{dw} < 50°C	$T_{mat} = 5.906 T_{dw}^{0.372} P^{0.508}$ (5)
15.2	Air	• Material in contact with canister bottom • 10 W < P < 20 W • 25°C < T_{dw} < 50°C	$T_{mat} = 6.945 T_{dw}^{0.325} P^{0.509}$ (6)
15.2	Helium	• Material in contact with canister bottom • 10 W < P < 20 W • 25°C < T_{dw} < 50°C	$T_{mat} = 3.190 T_{dw}^{0.539} P^{0.428}$ (7)
13.3	Air	• Material insulated from canister bottom • P = 15 W • 25°C < T_{dw} < 50°C	$T_{mat} = 0.940 T_{dw} + 75.3$ (8)
13.3	Helium	• Material insulated from canister bottom • P = 15 W • 25°C < T_{dw} < 50°C	$T_{mat} = 0.971 T_{dw} + 47.0$ (9)
8.9	Air	• Material insulated from canister bottom • P = 10 W • 25°C < T_{dw} < 50°C	$T_{mat} = 1.131 T_{dw} + 54.4$ (10)
8.9	Helium	• Material insulated from canister bottom • P = 10 W • 25°C < T_{dw} < 50°C	$T_{mat} = 1.042 T_{dw} + 39.1$ (11)

* Units for T_{dw} and P are degrees Celsius and watts, respectively.

3.4 Validation and Use of Empirical Correlations

To test the validity and robustness of the empirical correlations, material temperatures predicted with Equation (6) were compared to material storage temperature measurements from full-scale drywell thermal experiments [3, 5]. Equation (6) was selected because the material, nested canister, and fixture plate configurations used to develop the correlation were identical to those used in the full-scale drywell thermal tests.

As Figure 8 indicates, the material temperature predictions of Equation (6) agree quite well with the temperature measurements reported in References 3 and 5. The data used to construct and test the correlation lie within a ±10% error band. The material temperature predictions and measurements are also compared in Table 3, which indicates that the material temperature predictions are typically within a few degrees Celsius of the measured values. These differences can be attributed to thermocouple error and curve-fitting limitations.

Table 3. Comparison of measured [5] and predicted [Equation (6)] material temperatures for a full-scale drywell under different storage conditions.

Test Conditions [5]	Measured Drywell Temperature (°C) [5]	Measured Material Temperature (°C) [5]	Predicted Material Temperature (°C) using Equation (6)	Absolute Difference in Measured and Predicted Material Temperatures (°C)
• 5 Cans at 10 W each	24.1	62.6	63.1	0.5
	23.8	62.5	62.8	0.3
• 10 Cans at 10 W each	24.0	61.7	63.0	1.0
	24.0	60.3	63.0	2.7
	23.1	60.2	62.2	2.0
• 5 Cans at 15 W each	25.1	80.5	78.6	1.9
	24.4	80.0	77.8	2.2
• 10 Cans at 15 W each	26.8	83.8	80.3	3.5
	26.4	80.7	79.9	0.8
	24.7	80.3	78.2	2.1
• 10 Cans at 15 W each	46.4	99.3	95.9	3.4
	44.9	96.3	94.9	1.4
• Elevated Air Temp.	35.1	92.6	87.6	5.0

The successful validation of Equation (6) lends credibility to employing the empirical correlations of Table 2 to predict the upper limits of the material storage temperatures. In all practicality, a conservative mass heat-generation rate for aged plutonium metal of 2.8 W/kg will be acceptable for the NMSF. In this case, Equations (8) and (9) are appropriate for predicting the upper limit of the material storage

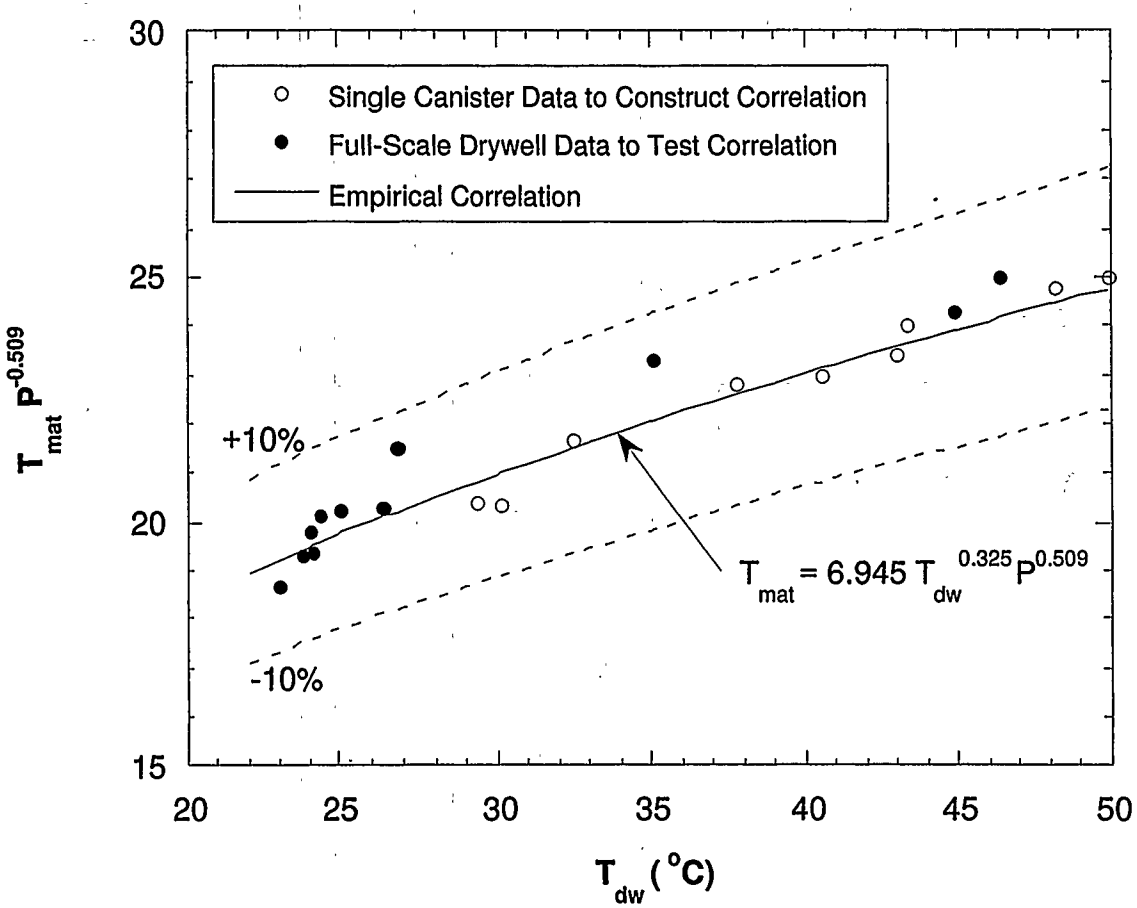

Figure 8. Correlation of the material storage temperature [Equation (6)].

temperatures for the maximum designed total heat-generation rate of 15 W per canister. If the storage design limits are reduced to 10 W per canister, then Equations (10) and (11) should be employed. For a given total heat-generation rate, the canister fill gas must be known in order to select the correct correlation. The use of helium rather than air as the canister fill gas will result in lower material storage temperatures. However, helium can slowly leak out of well-sealed canisters over time (and be replaced by the external gas, in this case air), thereby reducing the thermal performance of the storage system. Consequently, it may be more conservative to use the correlations corresponding to the air fill gas when predicting material storage temperatures.

In summary, to use Equations (8) through (11) to predict material storage temperatures, the total material heat-generation rate, canister fill gas, and drywell temperature in the vicinity of the canister must be known.

As a final note, if storage conditions vary from those used in this study (i.e., the mass heat-generation rate of the material differs from 2.8 W/kg, the canister fill gas is not air or helium, the fixture plate design changes, etc.), the empirical correlations may still be used in an intelligent fashion to interpolate or extrapolate material storage temperatures. However, great caution should be exercised to ensure that the temperature predictions are conservative.

4. CONCLUSIONS

An experimental study was performed to investigate the heat transfer characteristics of a material storage scheme for the Nuclear Materials Storage Facility and to develop empirical models to predict material storage temperatures. The key findings of this study are as follows:

1. The general heat dissipation characteristics of the nested canister storage configuration were presented with the aid of a temperature contour plot. Most of the thermal resistance is between the material and the inner canister.
2. A parametric study of influential variables revealed that the material storage temperature decreased with decreasing mass heat-generation rate, decreasing the

molecular weight of the canister fill gas, decreasing external (to drywell) air temperature, and reducing the thermal contact resistance between the material and the inner canister.

3. Empirically based models were developed to predict material temperatures under various storage conditions, and guidelines were provided to aid in implementing these correlations.
4. The validity, robustness, and implementation of the empirical correlations were demonstrated by comparing material temperature predictions with temperature measurements from full-scale drywell thermal experiments [3, 5]. Comparisons revealed that the material temperature predictions agreed to within a few degrees Celsius of the temperature measurements.

REFERENCES

[1] Bernardin, J. D., Hopkins, S., Gregory, W. S., and Martin, R. A., 1998, "A CFD Analysis and Experimental Investigation to Support the Design of Canister Holding Fixtures for the Los Alamos Nuclear Materials Storage Facility," *Proceedings of the 1998 ASME Fluids Engineering Division Summer Meeting,* Washington D. C.

[2] Bernardin, J. D., Hopkins, S., Gregory, W. S., Parietti, L., Bultman, D. L., and Martin, R. A., 1997, "CFD Analysis and Experimental Investigation associated with the Design of the Los Alamos Nuclear Materials Storage Facility," *Proceedings to the 1997 ASME Fluids Engineering Division Summer Meeting,* Vancouver, B.C., Canada.

[3] Bernardin, J. D., Hopkins, S., Chen, Z., Luck, D., Naffziger, D., and Gregory, W., 1997, "FY 1997 Experimental and Analytical Thermal Analysis of the Nuclear Materials Storage Facility," Technical Report LA-UR-97-4262, Los Alamos National Laboratory.

[4] Bernardin, J. D., Naffziger, D. C., and Gregory, W. S., 1997, "Experimental Assessment of the Thermal Performance of Storage Canister/Holding Fixture Configurations for the Los Alamos Nuclear Materials Storage Facility," Technical Report LA-13376-MS, Los Alamos National Laboratory.

[5] Hopkins, S., Gregory, W., and Bernardin, J., 1998, "NMSF Drywell Heat Transfer Experiments with Prototype Canister Holding Fixtures," Technical Report, LA-UR-98-2127, Los Alamos National Laboratory.

Appendix

Tables A.1 through A.5 contain all of the temperature data taken during the present study.

Table A.1. Temperature data from the single nested canister experiment with an aluminum cylinder (Length = 15.24 cm, O.D. = 5.08 cm) insulated from the inner canister by a G-10 spacer.

Test #	3	4	5	6	7	8	9	10	11	12	13	14	15	16	17	18	19	20	21
Can Spacing (cm)	30.5	30.5	30.5	30.5	30.5	30.5	30.5	30.5	30.5	30.5	30.5	30.5	30.5	30.5	30.5	30.5	30.5	30.5	30.5
Power (W)	15	15	10	10	15	15	15	10	15	15	15	10	15	20	20	20	10	10	20
Canister Gas	Air	Air	Air	Air	Air	Air	He	He	He	He	He	Air	Air	Air	Air	He	He	He	He
External Air Temp. Level	Low	Low	Low	Med	Med	High	Low	Low	Med	High	High	High	High	High	Low	Low	Med	High	High
Measurement Location (T.C. #)	Temperature (°C)																		
Material #1 (2)	93.4	94.6	74.0	79.5	.100.9	100.9	81.0	64.9	91.6	89.5	93.4	83.1	107.1	128.1	112.4	96.2	68.4	74.6	112.1
Material #2 (1)	94.6	95.9	74.8	80.5	102.3	102.3	83.2	66.4	93.5	91.8	95.5	84.1	108.4	129.9	114.1	98.8	69.8	76.2	114.8
Inner can top (3)	61.7	63.2	51.0	56.3	69.0	69.2	60.1	49.4	68.7	68.9	72.1	61.0	75.9	89.0	73.3	69.3	53.2	59.5	85.5
Inner can side (4)	45.9	47.5	39.8	45.4	53.4	53.9	47.8	41.3	55.8	58.2	60.4	50.7	61.4	70.5	53.9	53.2	44.7	52.4	70.6
Inner can bottom (5)	40.1	41.6	35.9	41.4	47.8	48.3	43.0	38.3	50.8	53.6	55.8	46.9	55.8	63.6	47.0	47.1	41.4	49.7	64.8
Inner can gas (6)	64.9	66.4	53.5	59.1	72.6	72.8	64.3	52.8	73.4	72.6	76.4	63.7	79.6	93.3	77.2	75.0	56.3	62.3	90.8
Outer can top (7)	45.7	47.2	39.8	45.2	53.0	53.4	48.6	42.2	54.5	56.2	58.5	48.5	57.8	65.7	48.7	49.7	43.2	50.5	67.3
Outer can side (8)	43.5	45.1	38.2	43.8	51.2	51.6	46.3	40.4	54.3	56.9	59.1	49.2	58.9	67.4	50.7	51.2	43.7	51.4	68.7
Outer can bottom (9)	37.6	39.2	34.2	39.7	45.3	45.7	40.9	36.9	48.7	51.5	53.7	45.0	53.1	60.0	43.3	44.3	39.7	48.1	62.1
Drywell (10)	26.9	28.4	26.3	31.4	33.9	34.9	29.7	28.8	37.8	40.9	42.7	37.3	42.2	46.2	29.8	31.0	31.8	39.9	48.4
Bottom fixture center (11)	36.5	38.0	33.4	38.9	44.1	44.5	39.9	36.3	47.8	50.5	52.8	44.3	52.2	58.7	42.2	43.3	39.1	47.5	61.0
Bottom fixture middle (12)	36.0	37.6	33.1	38.7	43.7	44.2	39.6	36.0	47.4	50.3	52.6	44.3	51.9	58.3	41.6	42.7	38.9	47.4	60.6
Bottom fixture edge (13)	35.4	37.1	32.6	38.2	43.1	43.7	38.9	35.6	46.8	49.6	51.9	43.8	51.2	57.5	40.9	41.9	38.5	46.9	59.8
Top fixture center (14)	36.7	37.8	34.3	38.3	43.4	44.0	40.8	37.0	48.1	50.3	52.5	45.2	51.9	57.8	38.3	41.5	42.7	48.0	62.1
Top fixture edge (15)	35.5	37.0	33.1	37.6	42.4	43.2	39.3	35.9	46.9	49.4	51.5	44.5	51.0	56.7	37.1	40.0	41.4	47.3	60.8
Air inside drywell #1 (16)	32.4	34.2	30.3	35.6	39.9	40.6	35.2	32.5	43.8	46.6	48.6	41.9	48.2	53.5	35.2	37.0	37.0	44.5	56.1
Air inside drywell #2 (17)	31.2	32.4	29.3	34.6	38.2	38.9	34.4	32.2	41.9	45.2	47.0	40.5	46.4	51.5	35.2	36.5	34.9	43.2	53.7
Air outside drywell #1 (18)	25.8	26.5	25.6	30.6	32.7	33.8	28.6	28.1	36.6	40.1	41.6	36.6	41.0	44.8	28.6	29.3	31.3	39.2	46.9
Air ouside drywell #2 (19)	25.6	26.9	25.0	31.1	33.4	34.5	28.3	28.0	37.5	41.2	42.7	37.7	42.2	46.2	27.9	29.0	31.9	40.1	48.4
Lab Air	23.3	23.8	23.7	23.8	22.7		25.1	25.5	25.3	25.7	25.0	25.0	24.8	25.8	25.7	26.3	25.9	26.1	27.1

Table A.2. Temperature data from the single nested canister experiment with an aluminum cylinder (Length = 15.24 cm, O.D. = 5.08 cm) in direct contact with the inner canister.

Test #	22	23	24	25	26	27
Can Spacing (cm)	30.5	30.5	30.5	30.5	30.5	30.5
Power (W)	15	10	20	15	15	10
Canister Gas	Air	Air	Air	Air	He	He
External Air Temp. Level	Low	Low	Low	Mid	Low	Low
Measurement Location (T.C. #)	Temperature (°C)					
Material #1 (2)	82.5	66.0	95.8	92.1	65.0	54.3
Material #2 (1)	83.1	66.5	96.5	92.7	67.0	55.6
Inner can top (3)	55.7	47.0	61.2	65.1	48.4	42.4
Inner can side (4)	48.2	41.7	51.8	58.4	46.0	41.5
Inner can bottom (5)	47.9	41.5	51.7	58.3	47.2	42.5
Inner can gas (6)	59.4	49.4	68.1	70.7	49.2	42.9
Outer can top (7)	46.5	40.5	50.6	57.6	45.2	40.6
Outer can side (8)	45.3	39.5	49.5	56.6	45.1	41.0
Outer can bottom (9)	42.4	37.5	45.9	53.9	44.3	40.5
Drywell (10)	31.8	29.7	32.6	43.1	32.5	31.6
Bottom fixture center (11)	41.5	37.0	43.9	52.3	43.0	39.4
Bottom fixture middle (12)	41.0	36.8	43.2	51.9	42.3	39.0
Bottom fixture edge (13)	40.3	36.2	42.5	51.4	41.7	38.6
Top fixture center (14)	41.0	38.1	43.0	53.9	43.1	40.9
Top fixture edge (15)	39.0	36.6	41.2	52.3	41.1	38.9
Air inside drywell #1 (16)	36.0	33.1	38.0	48.2	37.1	35.7
Air inside drywell #2 (17)	35.6	32.4	37.1	46.8	36.5	34.8
Air outside drywell #1 (18)	30.1	28.2	31.1	41.5	31.0	30.5
Air ouside drywell #2 (19)	30.3	29.0	31.5	42.7	31.4	30.5
Lab Air	26.8	26.3	27.0	28.0	27.0	27.5

Table A.3. Temperature data from the single nested canister experiment with an aluminum cylinder (Length = 15.24cm, O.D. = 5.08 cm) in direct contact with the inner canister.

Test #	28	29	30	31	32	33	34	35	36	37	38	39	40	41	42	43	44	45
Can Spacing (cm)	40.6	40.6	40.6	40.6	40.6	40.6	40.6	40.6	40.6	40.6	40.6	40.6	40.6	40.6	40.6	40.6	40.6	40.6
Power (W)	10	15	20	20	15	10	20	20	15	10	10	10	10	15	15	15	20	20
Canister Gas	Air	Air	Air	He	Air	Air	Air	Air	Air	Air	He	He	He	He	He	He	He	He
External Air Temp. Level	Low	Low	Low	Low	Mid	Mid	Mid	High	High	High	High	Mid	Low	Low	Mid	High	High	Mid
Measurement Location (T.C. #)	Temperature (°C)																	
Material #1 (2)	65.8	80.7	99.2	76.7	90.8	73.4	107.2	114.4	97.9	77.3	66.2	59.2	52.4	61.3	72.5	76.2	88.6	82.9
Material #2 (1)	66.1	81.2	100	79.4	91.3	74.0	108.1	115.5	98.7	77.9	67.7	60.6	53.7	63.5	74.6	78.2	91.3	85.7
Inner can top (3)	45.6	52.5	63.6	54.3	62.8	54.3	72.7	79.6	71.3	59.0	54.9	47.7	40.6	45.7	56.6	60.5	67.8	62.8
Inner can side (4)	40.8	45.3	53.7	49.3	56.1	49.6	63.3	70.4	64.4	54.8	52.9	46.7	39.7	43.9	53.5	57.9	64.4	60.1
Inner can bottom (5)	41.1	45.7	53.7	50.9	56.3	49.6	63.3	70.4	64.4	54.8	53.7	47.6	40.8	45.1	54.6	59.0	65.9	61.6
Inner can gas (6)	49.5	58.4	69.7	57.1	68.2	57.0	78.1	84.8	74.5	62.2	53.8	48.0	41.0	44.3	56.5	60.0	68.0	62.0
Outer can top (7)	39.8	43.7	50.8	47.4	54.5	47.8	60.7	67.7	62.3	53.1	51.2	45.6	38.5	41.3	51.6	55.8	62.0	57.4
Outer can side (8)	39.4	43.3	50.0	47.1	54.2	47.3	60.2	67.0	61.6	52.6	51.3	46.0	39.0	42.0	51.7	56.0	62.4	58.1
Outer can bottom (9)	37.8	41.0	46.5	45.8	51.6	45.4	56.6	63.4	58.9	50.8	50.6	45.4	38.7	41.4	50.9	55.4	61.5	57.1
Drywell (10)	29.3	30.1	32.5	32.0	40.5	37.8	43.0	49.9	48.2	43.3	42.9	36.8	30.1	30.2	39.7	44.2	46.4	42.0
Bottom fixture center (11)	37.0	39.7	45.3	44.9	50.3	44.9	55.2	62.2	58.1	50.4	50.3	44.6	37.9	40.8	50.1	54.5	60.1	55.8
Bottom fixture middle (12)	36.6	39.1	44.6	44.2	49.9	44.9	54.7	61.7	57.9	50.5	50.3	44.2	37.4	40.2	49.6	54.0	59.3	55.0
Bottom fixture edge (13)	36.1	38.6	43.9	43.4	49.2	44.4	53.8	60.8	57.1	49.8	49.6	43.8	37.0	39.5	48.8	53.3	58.4	54.1
Top fixture center (14)	38.7	40.5	44.2	44.1	52.7	50.4	56.3	63.8	61.3	55.1	54.5	45.8	37.3	40.5	54.4	58.1	60.6	56.3
Top fixture edge (15)	33.0	34.7	38.1	37.5	46.4	43.4	49.9	57.4	54.6	48.7	47.8	40.9	33.6	35.4	46.1	50.7	53.6	49.2
Air inside drywell #1 (16)	32.1	33.3	36.5	35.9	44.4	40.5	47.4	54.5	51.9	46.1	45.6	39.7	32.6	33.4	43.4	47.9	51.3	46.7
Air inside drywell #2 (17)	32.1	33.7	37.3	36.8	44.2	40.5	47.4	54.3	52.0	46.1	45.7	39.8	33.1	34.1	43.5	47.9	51.4	46.8
Air outside drywell #1 (18)	28.4	28.9	30.2	30.4	39.2	36.7	41.2	48.2	46.6	42.2	41.9	35.8	29.3	29.1	38.2	42.8	44.6	40.1
Air ouside drywell #2 (19)	29.2	30.0	32.3	31.9	41.1	38.0	42.7	50.2	48.6	44.1	43.8	36.5	28.7	29.5	39.8	44.8	46.6	41.7
Lab Air	25.5	26.3	26.0	27.0	26.0	26.8	27.0	27.5	27.5	27.0	27.0	27.0	27.0	26.5	26.0	25.5	24.0	24.0

Table A.4. Temperature data from the single nested canister experiment with an aluminum cylinder (Length = 13.3 cm, O.D. = 5.08 cm) insulated from the inner canister by a G-10 spacer.

Test #	46	47	48	49	50	51
Can Spacing (cm)	40.6	40.6	40.6	40.6	40.6	40.6
Power (W)	15	15	15	15	15	15
Canister Gas	Air	Air	Air	He	He	He
External Air Temp. Level	Low	Med	High	High	Med	Low
Measurement Location (T.C. #)	Temperature (°C)					
Material #1 (2)	100.4	108.4	114.0	88.1	80.0	74.2
Material #2 (1)	98.0	NA	NA	NA	NA	NA
Inner can top (3)	58.3	66.4	72.7	61.5	54.1	47.5
Inner can side (4)	45.6	54.2	60.9	58.2	51.4	43.6
Inner can bottom (5)	37.9	47.2	54.1	54.8	48.2	40.3
Inner can gas (6)	61.0	69.7	75.6	64.1	55.7	50.7
Outer can top (7)	43.7	52.9	59.4	56.2	49.2	41.5
Outer can side (8)	42.5	51.5	57.8	56.4	49.6	41.8
Outer can bottom (9)	34.7	43.7	50.2	51.9	45.2	37.3
Drywell (10)	26.9	34.7	41.4	41.9	34.9	27.6
Bottom fixture center (11)	33.3	42.1	48.7	50.6	43.9	36.0
Bottom fixture middle (12)	33.0	41.8	48.6	50.3	43.5	35.6
Bottom fixture edge (13)	32.5	41.3	48.0	49.6	42.9	35.0
Top fixture center (14)	33.1	43.5	50.8	50.9	43.2	34.9
Top fixture edge (15)	32.4	42.5	49.8	49.8	42.3	33.7
Air inside drywell #1 (16)	29.0	37.4	44.4	45.0	38.0	29.9
Air inside drywell #2 (17)	29.4	37.6	44.4	45.3	38.4	30.7
Air outside drywell #1 (18)	26.3	33.5	40.4	40.9	33.7	26.7
Air ouside drywell #2 (19)	25.9	34.5	42.0	42.3	34.7	26.6
Lab Air	24.0	24.0	25.0	25.3	24.0	24.3

Table A.5. Temperature data from the single nested canister experiment with an aluminum cylinder (Length = 8.9 cm, O.D. = 5.08 cm) insulated from the inner canister by a G-10 spacer.

Test #	52	53	55	56	57	58
Can Spacing (cm)	40.6	40.6	40.6	40.6	40.6	40.6
Power (W)	10	10	10	10	10	10
Canister Gas	Air	Air	Air	He	He	He
External Air Temp. Level	Low	Med	High	High	Med	Low
Measurement Location (T.C. #)	Temperature (°C)					
Material #1 (2)	87.3	90.8	98.2	78.7	72.9	66.1
Material #2 (1)	88.1	NA	98.8	79.4	73.6	66.7
Inner can top (3)	50.2	54.5	60.6	54.3	48.5	42.1
Inner can side (4)	42.9	48.1	51.7	50.0	43.8	37.4
Inner can bottom (5)	37.8	43.1	49.5	49.7	43.5	35.3
Inner can gas (6)	52.7	57.9	61.1	53.3	48.4	41.5
Outer can top (7)	40.7	46.1	50.6	49.0	42.9	36.6
Outer can side (8)	39.7	45.2	49.1	48.4	42.2	35.8
Outer can bottom (9)	34.8	40.5	44.3	45.6	39.0	32.7
Drywell (10)	28.4	33.8	37.8	38.1	32.2	26.0
Bottom fixture center (11)	34.1	39.5	43.3	44.7	38.3	32.0
Bottom fixture middle (12)	33.9	39.5	43.3	44.6	38.1	31.7
Bottom fixture edge (13)	33.5	39.1	42.7	44.1	37.7	31.5
Top fixture center (14)	34.8	41.6	47.0	45.1	38.2	31.8
Top fixture edge (15)	33.7	41.9	46.0	44.4	37.6	30.9
Air inside drywell #1 (16)	30.1	36.1	40.2	40.5	34.2	27.9
Air inside drywell #2 (17)	30.5	36.0	40.2	40.9	34.7	28.4
Air outside drywell #1 (18)	27.6	32.7	37.2	37.4	31.4	25.3
Air ouside drywell #2 (19)	27.6	33.6	39.0	38.9	32.1	25.6
Lab Air	25.5	24.5	24.5	24.0	24.5	23.8